

## The role of May vegetation greenness on the southeastern Tibetan Plateau for East Asian summer monsoon prediction

Jingyong Zhang,<sup>1</sup> Lingyun Wu,<sup>1</sup> Gang Huang,<sup>2</sup> Wenquan Zhu,<sup>3</sup> and Yan Zhang<sup>4,5</sup>

Received 21 September 2010; revised 11 December 2010; accepted 3 January 2011; published 5 March 2011.

[1] It is well known that the slowly varying oceanic processes provide the primary source for East Asian summer monsoon (EASM) predictability. However, the memory inherent in the land surface state is less well understood or applied toward the EASM prediction. Here we investigate the role of antecedent vegetation conditions over East Asia for the EASM variation and prediction using March, April, May, and spring mean satellite-sensed Normalized Difference Vegetation Index (NDVI) for the period of 1982–2006. Results show that May vegetation greenness on the southeastern Tibetan Plateau (TP) is most closely linked to the EASM, accounting for about half of the total EASM variance. May vegetation greenness on the southeastern TP has significant and positive correlations with summer rainfall over the southeastern TP, East Asian summer subtropical frontal region, and many areas of northern China. We further discuss the possible physical mechanism explaining our findings. It is proposed that increased TP vegetation greenness enhances surface thermal effects, which subsequently warm atmospheric temperature, as well as strengthen ascending motion, convergence at the lower layers and divergence at the higher layers, and summer monsoon circulation. Finally, a linear regression model is developed to predict the EASM strength by combination of El Niño–Southern Oscillation (ENSO) and the vegetation greenness. Hindcast for the period 1982–2006 shows that the use of the southeastern TP vegetation information can highly improve the EASM prediction skill compared to that using ENSO alone.

**Citation:** Zhang, J., L. Wu, G. Huang, W. Zhu, and Y. Zhang (2011), The role of May vegetation greenness on the southeastern Tibetan Plateau for East Asian summer monsoon prediction, *J. Geophys. Res.*, 116, D05106, doi:10.1029/2010JD015095.

### 1. Introduction

[2] The unique land–sea contrast and large-scale topography of the Tibetan Plateau produce the noted East Asian monsoon. During summer, the unusual behaviors of the East Asian monsoon may lead to occurrence of extensive drought/flood disasters in East Asia, which can cause serious consequences on the natural environment and the human society [e.g., *Tao and Chen*, 1987; *Ding*, 1992; *Lau and Weng*, 2001; *Huang et al.*, 2003]. Therefore, the accurate prediction of the East Asian summer monsoon (EASM) is of great

importance to sustainable development of East Asia. During the past 2 decades, many models and methods have been proposed to predict the EASM from the ocean forcing predictors such as El Niño–Southern Oscillation (ENSO) [e.g., *Cane et al.*, 1986; *Chang*, 2004; *Wang et al.*, 2005; *Wu et al.*, 2009], because the ocean is generally recognized to change slowly and have enormous heat content with a long climate memory. However, in some regions when the ENSO forcing is weak, such as the continental region during summer season, the models and methods show little skill [e.g., *Wang et al.*, 2009a]. Therefore, it is urgent to look for other potential sources to improve the EASM prediction skill.

[3] In addition to the ocean, land surface can also provide a critical memory function in the climate system at the monthly and longer time scales [*Shukla and Mintz*, 1982; *Yeh et al.*, 1984; *Koster and Suarez*, 1995; *Zhang et al.*, 2003a, 2008; *Wu and Dickinson*, 2004; *Liu et al.*, 2006]. It has been suggested to be an important factor in the modulation of the monsoon circulation, and therefore offers the potential for improving the EASM prediction [e.g., *Webster*, 1987; *Shukla*, 1998]. Vegetation, as a crucial parameter of the land surface, can influence climate on the local and regional to global scales through exchanges of energy, moisture and momentum

<sup>1</sup>Center for Monsoon System Research, Institute of Atmospheric Physics, Chinese Academy of Sciences, Beijing, China.

<sup>2</sup>LASG and RCE-TEA, Institute of Atmospheric Physics, Chinese Academy of Sciences, Beijing, China.

<sup>3</sup>State Key Laboratory of Earth Surface Processes and Resource Ecology, Beijing Normal University, Beijing, China.

<sup>4</sup>GEST, University of Maryland Baltimore County, Baltimore, Maryland, USA.

<sup>5</sup>Climate and Radiation Branch, NASA, Greenbelt, Maryland, USA.

between the land surface and the overlying atmosphere and resulted changes in regional and global atmospheric circulations [Pielke *et al.*, 1998; Pielke, 2001]. Significant interactions between vegetation and the monsoons have previously been recognized [e.g., Kutzbach *et al.*, 1996; Xue *et al.*, 2004; Castro *et al.*, 2009]. Our current understanding of how the vegetation affects the EASM and also the monsoons over other regions mainly comes from atmospheric models and numerical parameterization of Earth's land surface [Bonan, 2008]. For example, Xue *et al.* [2004] demonstrated that vegetation processes are among the most important mechanisms governing the EASM development, affecting its intensity, the spatial distribution of precipitation, and associated circulation at the continental scale. A recent GCM study estimated that vegetation interactions contribute to about 40% of the observed precipitation over the land, with the strongest effects in the monsoon regions including the EASM region [Xue *et al.*, 2010]. Numerical experiments also showed that human-induced land use and land cover changes in East Asia have brought significant influence on the EASM [e.g., Xue, 1996; Fu, 2003; Gao *et al.*, 2003; Cui *et al.*, 2006; Takata *et al.*, 2009]. In the early 2000s, Zhang *et al.* [2003a, 2003b] and Kaufmann *et al.* [2003] inferred vegetation effects on precipitation and/or temperature from observational records over China and the United States, respectively. Since then many researchers have made efforts to explore the role of vegetation in influencing surface climate using long-term satellite-sensed vegetation index and observational climate data [e.g., Liu *et al.*, 2006; Notaro *et al.*, 2006; Los *et al.*, 2006; Wang *et al.*, 2006; Hua *et al.*, 2008]. However, the role of vegetation in influencing the EASM is less well understood from the observations, and vegetation memory is less taken account into the prediction of the EASM.

[4] The objective of the study is to investigate the role of vegetation greenness for the EASM variation and prediction using satellite-sensed Normalized Difference Vegetation Index (NDVI) for the period of 1982–2006. We find that May NDVI on the southeastern Tibetan Plateau (TP) can account for 48% of the total EASM variance. We further discuss the possible physical mechanism to explain the finding, and finally apply May NDVI on the southeastern TP to improve the EASM prediction. This study significantly differs from our previous studies [Zhang *et al.*, 2003a, 2003b], which investigated the relationships of summer mean precipitation and temperature to previous winter and present spring mean NDVI over China. This study is also significantly different with recent several studies [e.g., Wang *et al.*, 2010; Zuo *et al.*, 2010], which used simultaneous correlations to investigate TP vegetation influences on China's rainfall. As pointed out by Liu *et al.* [2006], it is better to use the lagged relationship but not the simultaneous one to infer the vegetation influence since the vegetation growths are largely determined by climate. In addition, the simultaneous relationships cannot offer the potential for improving the seasonal prediction.

[5] This paper is organized as follows. Following a brief description of data and method used in section 2, we examine the relationships of March, April, May, and spring mean vegetation greenness over East Asia to the EASM in section 3. We identify a close relationship of EASM with May vegetation greenness on the southeastern TP. We further discuss, in section 4, the possible physical mechanism

explaining our findings. In section 5, an empirical model is established to predict the EASM by combination of ENSO and May vegetation greenness on the southeastern TP. Finally, conclusions are provided in section 6.

## 2. Data and Method

[6] NDVI is the difference between the Advanced Very High Resolution Radiometer (AVHRR) reflectance in near-infrared and visible bands divided by the sum of these two bands. We use 8-km-resolution Global Inventory Modeling and Mapping Studies (GIMMS) satellite drift corrected and NOAA-16 incorporated NDVI data for the period of 1982–2006 [Pinzon *et al.*, 2004; Tucker *et al.*, 2005]. The data record contains two 15 day composites for each month, the first for day 1 to 15, and the second for day 16 to the end of the month. Corrections performed to this data set reduced NDVI variations arising from calibration, view geometry, volcanic aerosols, and other effects not related to actual vegetation change. We aggregate the semimonthly 8-km-resolution data into  $1^\circ \times 1^\circ$  grid cells. Then, the monthly data are produced by using the higher value between two semimonthly data sets for each month.

[7] The circulation parameters rather than precipitation are commonly used to quantify the EASM strength due to the complex spatial and temporal structure of rainfall, and also a preference of using large-scale wind to define the broad-scale monsoon [Wang *et al.*, 2008b]. The EASM Index (EASMI) used in this study is a shear vorticity index which is defined by the U850 averaged in ( $22.5^\circ\text{N}$ – $32.5^\circ\text{N}$ ,  $110^\circ\text{E}$ – $140^\circ\text{E}$ ) minus U850 in ( $5^\circ\text{N}$ – $15^\circ\text{N}$ ,  $90^\circ\text{E}$ – $130^\circ\text{E}$ ), where U850 denotes the zonal wind at 850 hPa [Wang *et al.*, 2008b]. The simple index is the Wang and Fan [1999] index with a reversed sign. Wang *et al.* [2008b] recommended the index for monitoring the EASM after comparing 25 existing EASM indices because it has the best performance in capturing the total variance of the precipitation and three-dimensional circulation over East Asia, and it is nearly identical to the leading principle component of the EASM. The index physically reflects the variations in both the western North Pacific monsoon trough and subtropical high, which are the two key elements of the EASM circulation system [Tao and Chen, 1987; Wang *et al.*, 2008b]. It is closely associated with the leading EOF mode of the interannual variations in summer precipitation over East Asia ( $20^\circ\text{N}$ – $50^\circ\text{N}$ ,  $100^\circ\text{E}$ – $180^\circ\text{E}$ ) with a high correlation coefficient of 0.71 for the period of 1979–2004 [Lee *et al.*, 2005]. In the meanwhile, the EASMI, like any other index, has its potential limitations that should be recognized [Wang *et al.*, 2008b]. The EASMI is calculated using June-to-August mean zonal wind data from National Centers for Environmental Prediction (NCEP)–U.S. Department of Energy (DOE) Reanalysis II [Kanamitsu *et al.*, 2002]. The NCEP-DOE Reanalysis II data are also used to explore the possible physical mechanism explaining the close relationship between May vegetation greenness on the southeastern TP and the EASM.

[8] The monthly precipitation is obtained from the Climate Prediction Center (CPC) Merged Analysis of Precipitation (CMAP) data set for the same period at a  $2.5^\circ \times 2.5^\circ$  resolution [Xie and Arkin, 1997]. It is derived from rain gauge observations, satellite estimates, and National Centers for

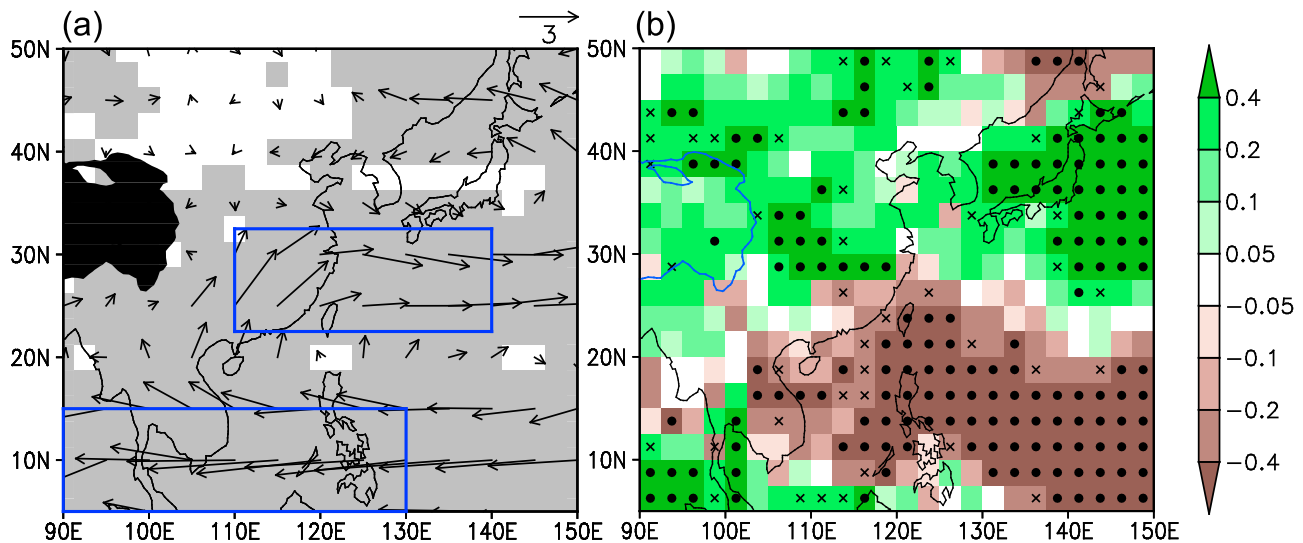


**Figure 1.** (a) Composite difference of summer 850 hPa horizontal wind vector (in  $\text{m s}^{-1}$ ) between the five highest and five lowest years of detrended EASM index (EASMI) for the period of 1982–2006. (b) Correlation pattern of summer CMAP precipitation with the EASMI for the period of 1982–2006. The EASMI is an inverse Wang-Fan index [Wang and Fan, 1999; Wang et al., 2008b] and is defined by the 850 hPa zonal wind difference averaged in the north box minus that in the south box. The precipitation and EASMI data are linearly detrended before the correlation coefficient is calculated. In Figure 1a, the values in the shaded areas are significant at the 90%  $t$  test confidence level. In Figure 1b, the grid cells passing the 90% and 95% confidence levels are marked by crosses and closed circles, respectively.

Environmental Prediction-National Center for Atmospheric Research (NCEP-NCAR) reanalysis.

### 3. May Vegetation Greenness on the Southeastern TP and the EASM

[9] Figure 1a presents composite difference of summer 850 hPa horizontal wind vector between the five highest and five lowest EASMI years. Strong EASM tends to result in enhanced southwesterly anomalies on the northwestern flank of the strengthened anticyclonic circulation over the western North Pacific and enhanced easterly anomalies over the tropical region. The EASMI is significantly and positively correlated with summer precipitation at many grid cells along a southwest-northeast oriented rain belt extending from the mid-lower reach of the Yangtze River valley across South Korea to eastern Japan, which is primarily along the East Asian subtropical front (called *Meiyu* in Chinese, *Changma* in Korean, and *Baiu* in Japanese). In addition, it exhibits significant and negative correlations with western North Pacific summer monsoon rainfall (Figure 1b). The results agree well with previous studies [Wang et al., 2008b; Wu et al., 2009].

[10] To investigate the relationship between the EASM and the spring vegetation greenness in East Asia, we calculate the correlation coefficients between the EASMI and March, April, May, and spring mean NDVI for the period 1982–2006, respectively. The results show that the EASMI has the strongest correlation with May NDVI on the southeastern TP (Figure 2a). We average May NDVI enclosed by the box ( $93^{\circ}\text{E}$ – $102^{\circ}\text{E}$ ,  $29^{\circ}\text{N}$ – $34^{\circ}\text{N}$ ) ( $NDVI_{MSTP}$ ) to represent May vegetation greenness on the southeastern TP. The southeastern TP is covered by evergreen broad-leaved forest, coniferous forest, shrub, and meadow [Zheng, 1996], which

can grow almost all the year around [Ding et al., 2007]. Compared to other areas of the TP, the annual mean albedo of the southeastern TP is low, with a value of 0.2–0.25 [Xu and Lin, 2002]. The 1982–2006 mean May NDVI averaged over the southeastern TP is 0.23, with values at almost all grid cells larger than 0.12 (Figure 2b). The NDVI is expressed on a scale from  $-1$  to  $+1$ . While the NDVI values between  $-0.2$  to  $0.1$  are for snow, inland water bodies, deserts and exposed soils, the values larger than  $0.1$  reflect the amounts of the green vegetation well [e.g., Tucker et al., 1986; Zhou et al., 2001]. This indicates that  $NDVI_{MSTP}$  can represent variation of May vegetation greenness well particularly when region-averaged NDVI is used to quantify the density of plant growth. Meanwhile, it needs to mention that the snow indeed exists in May on the southeastern TP, and thus can reduce the NDVI values to some degree (see Figure S1).<sup>1</sup> In addition, vegetation growth is largely affected by climatic factors such as soil moisture and soil temperature [e.g., Nemani et al., 2003]. Therefore, it should be kept in mind that the relationship between  $NDVI_{MSTP}$  and the EASMI may actually reflect combined effects of vegetation, soil, and snow over the southeastern TP on the EASM. Figure 2c shows that the variation of the EASMI is consistent with that of  $NDVI_{MSTP}$ . The correlation coefficient between them is 0.70, which is significant at the 99.9% confidence level by student's  $t$  test.

[11] Figure 3 shows correlation pattern of summer precipitation with  $NDVI_{MSTP}$ .  $NDVI_{MSTP}$  is significantly and positively correlated with summer precipitation over the southeastern TP, East Asian subtropical frontal region, and many areas of

<sup>1</sup>Auxiliary materials are available with the HTML. doi:10.1029/2010JD015095.

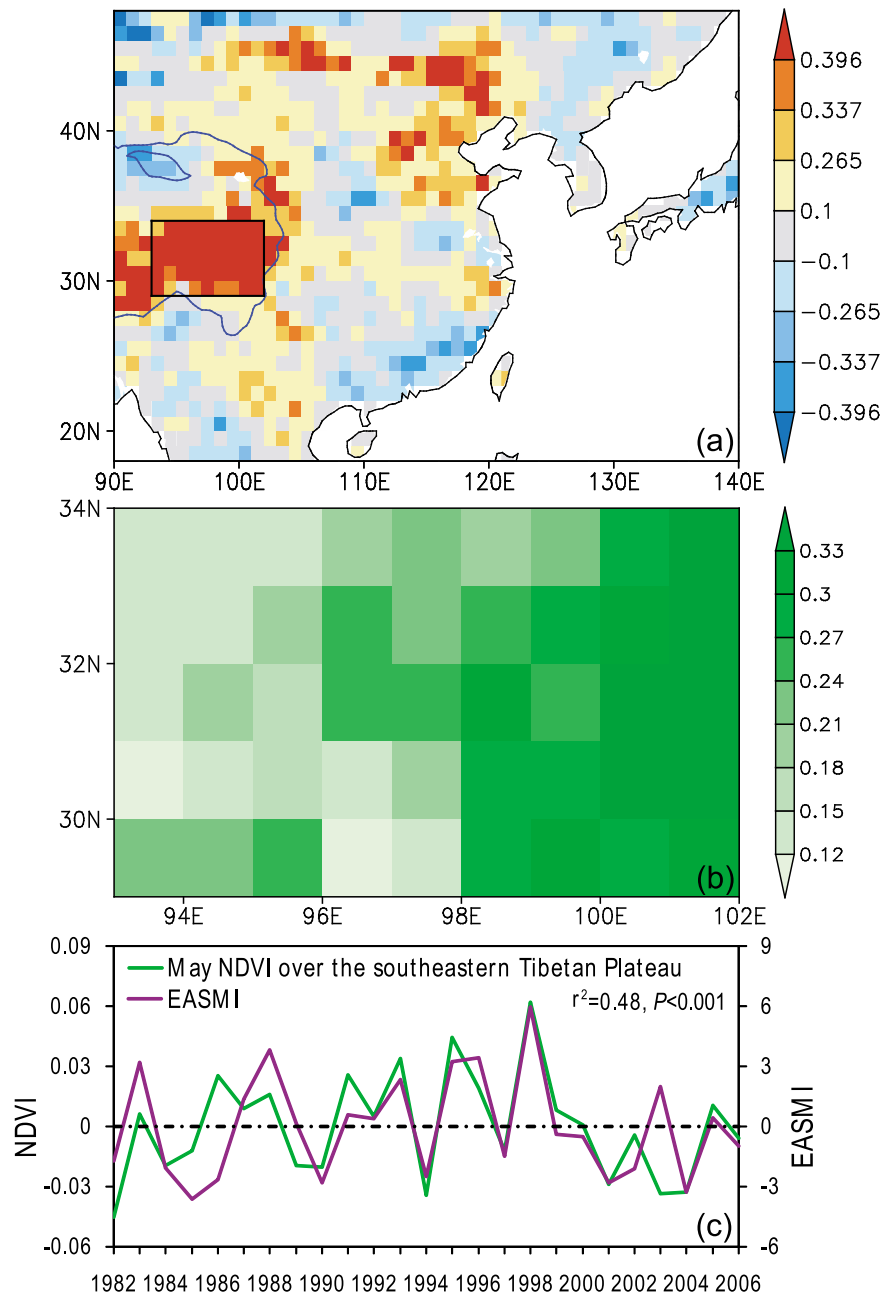


**Figure 2.** (a) Correlation pattern of May NDVI with the EASM index (EASMI) for the period of 1982–2006. (b) The 1982–2006 mean May NDVI on the southeastern Tibetan Plateau (enclosed by the box in Figure 2a). (c) Time series of the EASMI and May NDVI averaged over the southeastern Tibetan Plateau. The NDVI and EASMI data are linearly detrended before the correlation coefficient is calculated. Correlations of  $\pm 0.265$ ,  $\pm 0.337$ , and  $\pm 0.369$  are significant at the 80, 90, and 95% levels, respectively. The blue solid line in Figure 2a denotes the topographic contour line of 3000 m.

northern China. In addition, significant negative correlations mainly appear over western North Pacific summer monsoon region. These results indicate that increased vegetation greenness on the southeastern TP tends to result in increased summer rainfall over the southeastern TP, East Asian summer subtropical frontal region, and many areas of northern China, and decreased summer rainfall over western North Pacific summer monsoon region, and vice versa.

#### 4. Discussion of the Physical Mechanism

[12] The huge mechanical and thermal forcings of the TP that is a region of strong land-atmosphere interactions [e.g., Yanai and Wu, 2006; Xue *et al.*, 2010], exert profound influence on the climate over East Asia as well as over the globe [e.g., Ye and Gao, 1979]. Previous observational studies showed that increased vegetation greenness over southwestern China (including the southeastern TP) tends to reduce surface

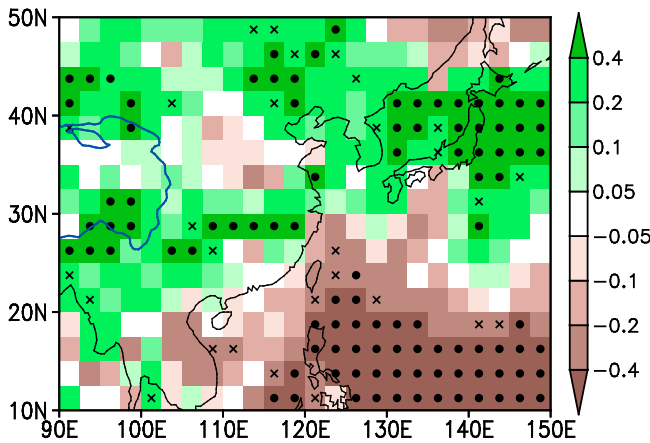


**Figure 3.** Correlation pattern of summer CMAP precipitation with May NDVI averaged over the southeastern Tibetan Plateau for the period of 1982–2006. The NDVI and precipitation data are linearly detrended before the correlation coefficient is calculated. The grid cells passing the 90% and 95% confidence levels are marked by crosses and closed circles, respectively. The blue solid line denotes the topographic contour line of 3000 m.

albedo, thus resulting in more energy absorption and the enhancement of the warming [e.g., Liu *et al.*, 2006]. Hua *et al.* [2008] investigated the relationships of vegetation greenness to surface energy balance components and temperatures on the TP using the station data from the Sino-Japanese Cooperation Research Project on Asian Monsoon Mechanism, the GEWEX Asian Monsoon Experiment in the Tibetan Plateau (GAME/Tibet) and the second Tibetan Plateau Meteorological Experiment (TIPEX). They found that increased vegetation greenness is accompanied by increased net shortwave radiation, net longwave radiation, sensible heat and latent heat, which may subsequently enhance ground and surface air temperatures. The enhancement of the warming by the vegetation also showed up in some other regions [e.g., Kaufmann *et al.*, 2003; Notaro *et al.*, 2006; Wang *et al.*, 2006]. Meanwhile, some numerical studies demonstrated that deforestations at midlatitudes have cooled Northern Hemisphere climate through biogeophysical effects [e.g., Bonan, 1997; Brovkin *et al.*, 1999, 2006; Betts, 2001; Bounoua *et al.*, 2002; Feddema *et al.*, 2005; Davin and de Noblet-Ducoudre, 2010].

[13] We examine the thermal effects of vegetation greenness on the southeastern TP using sensible and latent heat data from NCEP-DOE Reanalysis II (Figure 4). The NCEP-DOE reanalysis data have been demonstrated to reasonably reflect seasonal and annual variations of surface heat fluxes on the TP when compared to the station data from the Sino-Japanese Cooperation Research Project on Asian Monsoon Mechanism, the GAME/Tibet, and the second TIPEX [Hua *et al.*, 2008]. Variations of the NCEP-DOE reanalysis air temperature and radiation fluxes are also found to agree with those of observed data though the averaged temperature values were systematically lower than the observed ones due to the higher topography used in the reanalysis model [Wei and Li, 2003]. Figures 4a and 4b show composite differences of June–July mean surface latent and sensible heat fluxes between the 5 highest (1986, 1991, 1993, 1995, and 1998)

and 5 lowest (1982, 1994, 2001, 2003, and 2004) years of  $NDVI_{MSTP}$ . Increased May vegetation greenness on the southeastern TP tends to increase June–July latent and sensible heat fluxes by decreasing surface albedo and thus increasing the solar energy absorption. The increased surface heating subsequently results in increased surface air temperature with an average value of  $1.8^{\circ}\text{C}$  over the southeastern TP (Figure 4c). In August, the thermal effects of the vegetation become weak (not shown). We estimate the vegetation memory using the method given by Notaro *et al.* [2006] which calculated decorrelation time based on lag-1-month autocorrelation [von Storch and Zwiers, 1999]. The estimated memory is slightly longer than 2 months, and this may account for the weak thermal effects of the vegetation in August. The composite difference of longitude–height section of air temperature along  $32.5^{\circ}\text{N}$  between the five highest and five lowest years of  $NDVI_{MSTP}$  shows that positive temperature anomalies are significant at the 90% confidence level both at the surface and in the troposphere, with the magnitude of the order of  $0.5^{\circ}\text{C}$ – $2^{\circ}\text{C}$  (Figure 4d). At the levels between 200 and 400 hPa, significant positive anomalies of air temperature extend eastward to around  $130^{\circ}\text{E}$ . The elevated heating on the TP mainly depends on sensible heating at surface layers, while the deep condensation heating becomes dominant at the higher layers [e.g., Wu *et al.*, 2005; Duan and Wu, 2005]. Therefore, the increased atmospheric temperature may reflect combined effects of sensible heating and condensation heating. At the lower layers, the warming may be directly caused by increased sensible heating. This subsequently enhances vertical ascending motion, and makes more atmospheric moisture precipitate out and enhances condensation heating at the higher layers. The above analysis indicates that increased vegetation greenness on the southeastern TP tends to increase the temperature both at the surface and in the troposphere through its direct effect on surface sensible heating and indirect effect on condensation heating.

[14] Several previous studies have related surface sensible and latent heat fluxes to vegetation variations on the TP [e.g., Hua *et al.*, 2008; Wang *et al.*, 2010; Zuo *et al.*, 2010]. Based on the analysis of the observations, Hua *et al.* [2008] found that the NDVI changes on both eastern and western TP have positive correlations with surface sensible heat and latent heat fluxes, which is consistent with our analysis. Using the reanalysis data, Wang *et al.* [2010] and Zuo *et al.* [2010] obtained different relationships between surface heating and vegetation during spring and summer, i.e., the enhancement of surface sensible heating by an increase in vegetation on the TP during spring, and an increase in summer vegetation accompanied by a decrease in the amount of summer sensible heat and latent heat around the southern TP. The negative effects of vegetation on surface heating found by Zuo *et al.* [2010] appear to be inconsistent with those from Hua *et al.* [2008] and this study.

[15] To test if our results depend on the choice of the sample number, we compute composite differences between the six highest and six lowest years of  $NDVI_{MSTP}$ , and between the seven highest and seven lowest years in surface heat fluxes and also in circulation parameters. The results are generally consistent with the composite differences between the five highest and five lowest years. Therefore, in the following analyses, we only show and discuss the composite differences between the five highest and five lowest years.

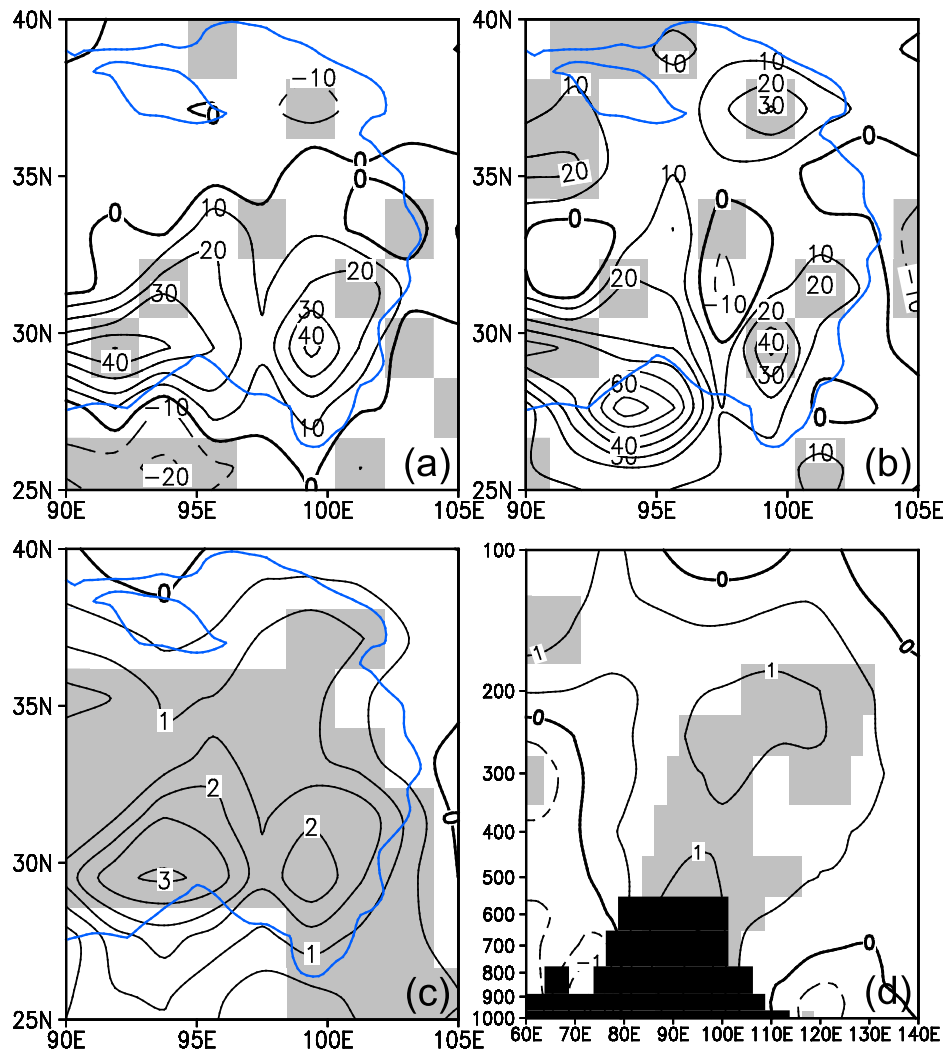


**Figure 4.** Composite differences of June–July mean surface latent and sensible heat fluxes (in  $\text{W m}^{-2}$ ) and air temperature (in  $^{\circ}\text{C}$ ) between the five highest and five lowest years of detrended May NDVI on the southeastern Tibetan Plateau: (a) surface latent heat, (b) surface sensible heat, (c) surface air temperature, and (d) cross section of air temperature along  $32.5^{\circ}\text{N}$ . The values in the shaded areas are significant at the 90%  $t$  test confidence level. The blue solid line denotes the topographic contour line of 3000 m.

[16] The thermal forcing of the TP plays an important role in influencing summer atmospheric circulation over East Asia, as well as over the Northern Hemisphere [e.g., *Ye and Gao, 1979; Tao and Chen, 1987; Wu et al., 1997; Zhao and Chen, 2001; Yanai and Wu, 2006; Liu et al., 2007; Wang et al., 2008a; Ma et al., 2009*]. We subsequently look at changes in East Asian atmospheric circulation system associated with the thermal effects of the vegetation on the southeastern TP. Figure 5 shows composite differences of summer 100 and 850 hPa horizontal wind vector between the five highest and five lowest years of  $NDVI_{MSTP}$ . With intensified South Asian high, increased vegetation greenness on the southeastern TP tends to enhance deep and strong anticyclonic circulation at the higher layers. At 850 hPa, corresponding to the high years of  $NDVI_{MSTP}$ , an anomalous anticyclone is found over South China and the western North Pacific with the expanded western North Pacific subtropical high while an anomalous cyclone is observed in the northern part of East Asia and adjacent ocean. They together result in

the increased southwesterlies along northwestern flank of the low-level anticyclonic circulation over the western North Pacific, which increase water vapor transport toward East Asian subtropical front. In addition, the anomalous cyclone leads to anomalous easterlies over Northeast China and anomalous northerlies over North China.

[17] In summer, the TP acts as a strong heat source, with the larger thermal effects in the lower layers. *Duan and Wu [2005]* found that according to the large-scale quasi-steady vorticity equation, airflows must converge at lower layers and diverge at higher layers on the east of the TP, and bring opposite conditions to its west. This subsequently causes ascending motion on the east and descending motion on the west. Corresponding to the high years of  $NDVI_{MSTP}$ , significant anomalous ascending motion appears over the southeastern TP, East Asian summer subtropical frontal region, and many areas of northern China while significant anomalous descending motion is seen over the western North Pacific (Figure 6a). The composite difference of the

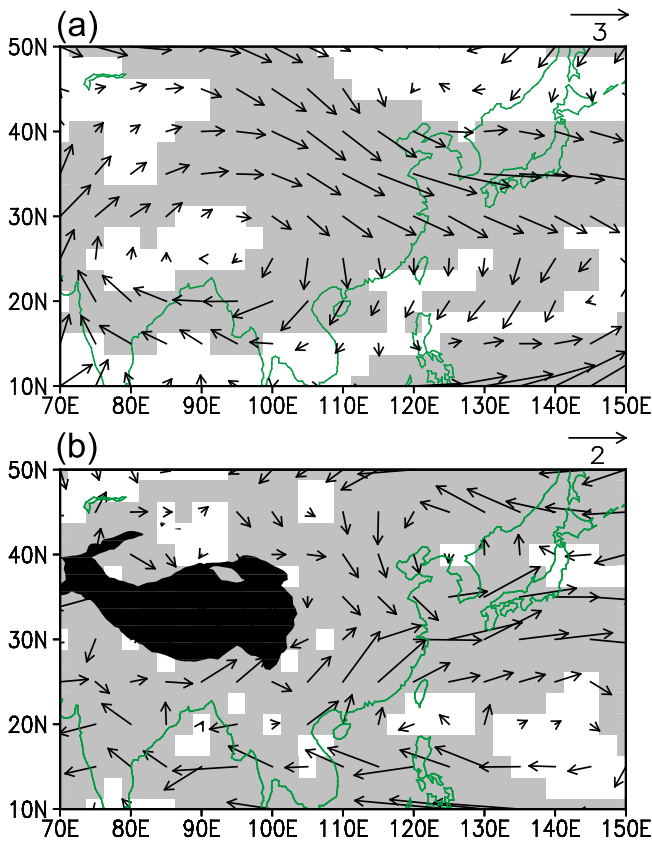


**Figure 5.** Composite difference of summer (a) 100 and (b) 850 hPa horizontal wind vector (in  $\text{m s}^{-1}$ ) between the five highest and five lowest years of detrended May NDVI on the southeastern Tibetan Plateau. The values in the shaded areas are significant at the 90%  $t$  test confidence level.

cross section of vertical motion along  $30^\circ\text{N}$  shows that increased vegetation greenness on the southeastern TP tends to enhance ascending motion on its east and descending motion on its west (Figure 6b). Particularly, anomalous values on its east are significant at the 90% confidence level both at surface layers and in the whole troposphere. From the composite difference of the cross section of vertical motion along  $95^\circ\text{E}$  (Figure 6c), significant negative anomalies on the southeastern TP are accompanied by positive anomalies on its southern and northern sides. These results indicate that increased vegetation greenness on the southeastern TP tends to enhance the ascending (descending) motion over the southeastern TP, East Asian subtropical frontal region, and many areas of northern China (over the western North Pacific).

[18] Composite differences of summer 200 hPa and 850 hPa divergences between the five highest and five lowest years of  $NDVI_{MSTP}$  anomalies show that corresponding to the high years of  $NDVI_{MSTP}$ , there are generally more divergence at the upper level and more convergence at the lower level over the southeastern TP, East Asian summer subtropical frontal region, and many areas of northern China (Figure 7). This suggests that greener vegetation on the southeastern TP is followed by more divergence at the upper level and more convergence at the lower level over these areas. Increased southeastern TP vegetation greenness tends to bring the

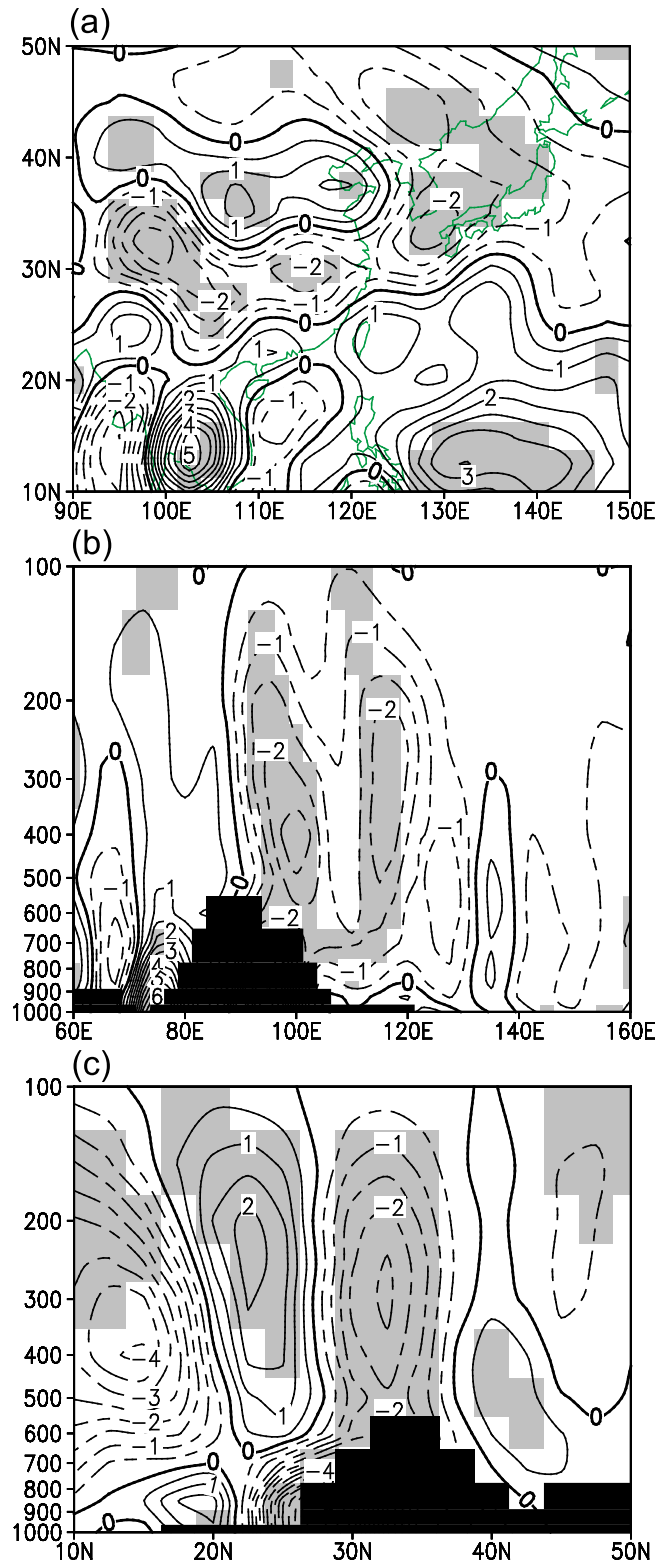


**Figure 6.** Composite difference of summer vertical motion (in  $10^{-2} \text{ Pa s}^{-1}$ ) between the five highest and five lowest years of detrended May NDVI on the southeastern Tibetan Plateau: (a) spatial distribution at 500 hPa, (b) longitude-height section along  $30^\circ\text{N}$ , and (c) latitude-height section along  $95^\circ\text{E}$ . The values in the shaded areas are significant at the 90%  $t$  test confidence level.

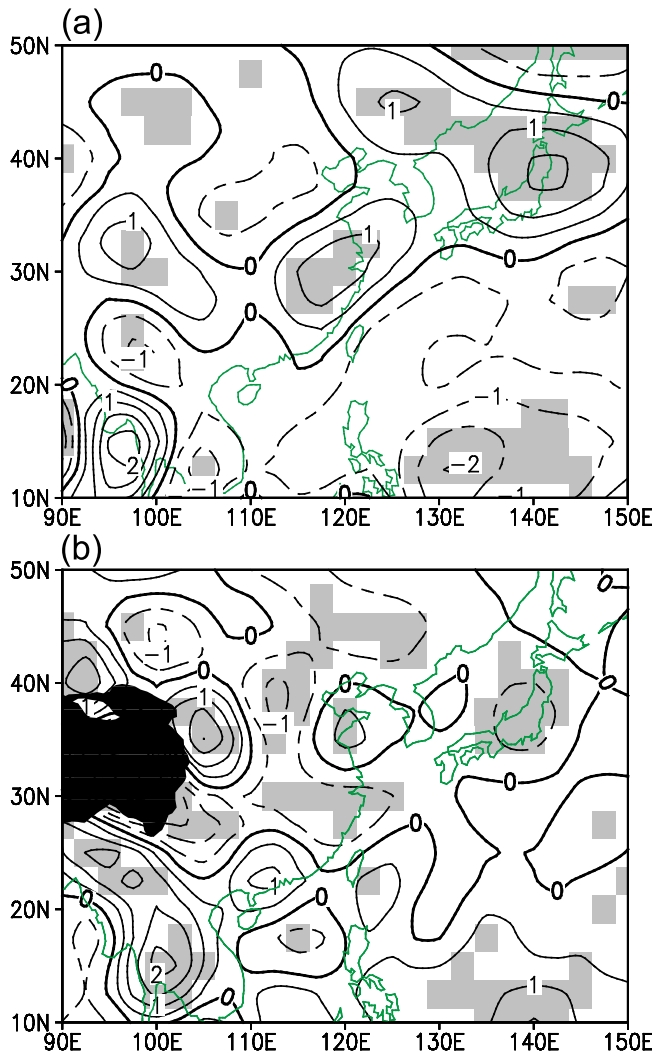


**Figure 7.** Composite difference of summer (a) 200 and (b) 850 hPa divergence ( $10^{-6} \text{ s}^{-1}$ ) between the five highest and five lowest years of detrended May NDVI on the southeastern Tibetan Plateau. Positive and negative values denote divergence and convergence, respectively. The values in the shaded areas are significant at the 90%  $t$  test confidence level.

opposite conditions to those mentioned above to the western North Pacific monsoon region.

[19] Oceanic processes and the snow may exert influences on both May vegetation greenness on the southeastern TP and the EASM, thus contributing to the close relationship between them. ENSO is the primary oceanic forcing factor that affects the EASM. We further calculate partial correlations of  $NDVI_{MSTP}$  with the EASMI adjusted for previous winter (December-to-February) Niño3.4 index, spring (March-to-May) Niño3.4 index, and the Niño3.4 index difference between April–May and February–March (the former minus the latter). They are 0.65, 0.67, and 0.67, slightly smaller than the simple correlation coefficient of 0.70. This suggests that ENSO makes a limited contribution to the relation between  $NDVI_{MSTP}$  and the EASM. In addition, other oceanic processes such as Indian Ocean sea surface temperature (SST) and North Atlantic oscillation

(NAO) may also play a role, although they are less important to affect the EASM compared to ENSO [e.g., Yang et al., 2007; Xie et al., 2009; Wu et al., 2009].

[20] The snow is another land surface factor that can affect the Asian monsoon system [e.g., Hahn and Shukla, 1976; Chen and Yan, 1979]. Some studies demonstrated that winter-spring Tibetan snow is positively related with summer rainfall over the mid-lower reach of the Yangtze River valley [e.g., Wu and Qian, 2003; Qian et al., 2003; Zhang et al., 2004]. However, the correlations between the winter-spring Tibetan snow and summer rainfall over China are normally found to be relatively low or moderate in previous studies [e.g., Qian et al., 2003; Zhang et al., 2004], and the physical connection between them is still unclear [Yanai and Wu, 2006]. Recent studies found that there is no significant relationship between the winter-spring Tibetan snow with the intensity of summer monsoon, which is in contradiction to previous studies [Wu and Kirtman, 2007; Xu and Li, 2010]. Ueda et al. [2003] demonstrated that surface air temperature anomalies produced during the snow disappearance period diminished in May, suggesting that the dynamical linkage between the snow and the monsoon is weak. In addition, the winter snow is found to enhance the vegetation growth during the growing seasons, but only can account for 14% or less of the variance of the vegetation [Peng et al., 2010]. We further investigate spatial distribution of May snow cover using MODIS snow cover fraction data for the period of 2000–2010 (see Figure S1). Snow cover fractions in May are generally smaller than 15% on the southeastern TP except for its southwestern part ( $29^{\circ}\text{N}$ – $31^{\circ}\text{N}$ ,  $93^{\circ}\text{E}$ – $98^{\circ}\text{E}$ ). Snow cover fractions depend on the topography and location on the southeastern TP and also the other areas of the TP [Xu and Li, 2010]. For every individual year, spatial pattern of May snow cover is very similar. Therefore, the difference in spatial pattern of May snow cover averaged over the period of 2000–2010 and averaged over the study period should be small. The correlation coefficient of the EASMI with  $NDVI_{MSTP}$  is 0.70 after removing these grid cells on the southwestern part of the southeastern TP. As mentioned in section 3, the NDVI values lower than 0.1 are for snow, inland water bodies, deserts and exposed soils. We also calculate the correlation coefficient between the EASMI and  $NDVI_{MSTP}$  after only removing the two grid cells with the NDVI values lower than 0.12 (Figure 2b), which is 0.69. The two correlation coefficients almost have no change compared to that calculated using all grid cells on the southeastern TP, suggesting that May snow plays a very limited role in influencing the relationship between  $NDVI_{MSTP}$  and the EASMI. In summary, the above analyses suggest that the snow cannot contribute much to the correlation between  $NDVI_{MSTP}$  and the EASMI.

## 5. Seasonal Prediction of the EASM

[21] With a high correlation of 0.70 with the EASMI,  $NDVI_{MSTP}$  provides a useful predictor for the EASM, although the close relationship may include signals from the effects of oceanic processes and the snow. On the other hand, ENSO is previously recognized as a dominant predictor of the EASM [e.g., Fu and Teng, 1988; Huang and Wu, 1989; Weng et al., 1999; Wang et al., 2000]. Lee et al. [2008] took an

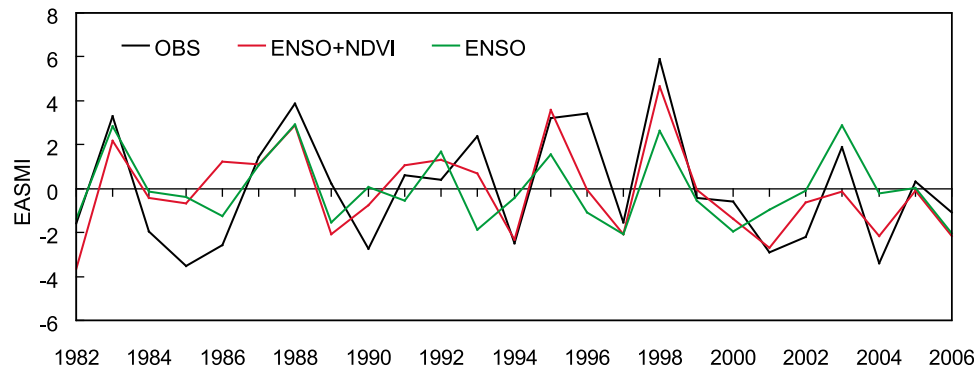


**Figure 8.** Time series of observed and hindcasted EASMI for the period of 1982–2006.

attempt to use both land surface conditions and ocean heat sources to predict East Asian summer rainfall, and demonstrated that land cover conditions are of importance in improving the predictive skills in their prediction models. Here, we develop an empirical prediction model of the EASMI based on ENSO and  $NDVI_{MSTP}$  using a linear regression for the period of 1982–2006. Since the linear trends almost do not change the correlation between  $NDVI_{MSTP}$  and the EASMI (0.70 versus 0.69 with and without the linear trend removed), we use original time series of ENSO,  $NDVI_{MSTP}$ , and EASMI to develop the empirical model:

$$EASMI = -14.95 + 52.84(NDVI_{MSTP}) - 2.07(ENSOI)$$

where  $ENSOI$  denotes the Niño3.4 index difference between April–May and February–March (the former minus the latter). Previous studies have demonstrated that ENSO can affect the EASMI not only on its decay phases but also on its development phases [e.g., Wang *et al.*, 2009b]. The ENSO index used in this study quantitatively measures both ENSO decay and development. The correlation coefficients of the EASMI with  $ENSOI$ , previous winter (December-to-February) Niño3.4 index, and present spring (March-to-May) Niño3.4 index are 0.63, 0.58, and 0.35, respectively. These results suggest that the ENSO index we use can be as a better predictor than the Niño3.4 indexes in previous winter and present spring. The correlation between the simulation and the observation of the EASMI is 0.81, indicating that the empirical model can simulate the EASMI variations quite well.

[22] To test the predictive capability of the empirical model, we utilize the cross-validation method to hindcast the EASMI. Cross-validation is a technique for estimating how accurately a predictive model will perform in practice [Stone, 1974; Efron and Tibshirani, 1993]. The data set is separated into two sets, called the training set and the testing set. In this study, we use fivefold cross-validation to estimate the EASMI. In the fivefold cross-validation, the data set is randomly divided into 5 subsets. Of the 5 subsets, a single subset is retained as the validation data for testing the model, and the remaining 4 subsets are used as the training data. The cross-validation process is then repeated 5 times, with each of 5 subsets used exactly once as the validation data. The reasons for using the fivefold cross-validation are twofold: (1) the hindcast period is 25 years, and the data can

be equally divided into five subsets; (2) 5 years is 20% of the whole data, and it falls into the range which can efficiently avoid overfitting or wasting data [e.g., Blockeel and Struyf, 2002]. Prediction skill is measured in terms of the square of the correlation coefficient ( $r^2$ ) between the observed time series of the EASMI and the corresponding cross-validation estimates. Figure 8 shows time series of the observed and hindcasted EASMI for the period of 1982–2006. When only ENSO is used in the empirical prediction model, the  $r^2$  value is 0.33, indicating that ENSO accounts for 33% of the observed EASMI variance. If May NDVI on the southeastern TP is included in the empirical prediction model, the  $r^2$  value increases to 0.58. This indicates that the use of May vegetation information on the southeastern TP does greatly improve the prediction skill of the empirical model. The empirical model is developed based on ENSO and  $NDVI_{MSTP}$ . In addition to ENSO, other oceanic processes such as the Indian ocean SST and NAO can also affect the EASMI. The inclusions of other oceanic forcing factors in the empirical model may add value to the prediction skill. The EASMI and also the monsoons over other regions have experienced significant multiple-decadal reductions [Chase *et al.*, 2003; Xu *et al.*, 2006], and the interannual relationship between the vegetation and the EASMI identified for the period of 1982–2006 may change should significant changes in the EASMI circulation occur in the future. In this study, we explore the role of May vegetation greenness on the southeastern TP for the prediction of mean EASMI strength, and how the vegetation (and also other land surface parameters) can improve the prediction of seasonal march of the EASMI needs further investigation in the future.

## 6. Conclusions

[23] The EASMI has complex space and time structures, therefore, its predictability and prediction have been a great challenge during the past years [e.g., Kang *et al.*, 2002; Huang *et al.*, 2003; Wang and Li, 2004; Ding and Chan, 2005; Wu *et al.*, 2009]. Most of previous research work linked the EASMI to anomalous SST. In particular, it is generally recognized that the EASMI is intimately associated with the ENSO variation. However, the land surface, another slowly varying climate component, is less well understood or applied toward the EASMI prediction. In this study, we investigated the role of

spring vegetation in East Asia for the EASM prediction using satellite-sensed NDVI and an inverse Wang-Fan EASM index [Wang and Fan, 1999; Wang et al., 2008b] for the period of 1982–2006. Results show that May NDVI on the southeastern TP is highly correlated with the EASMI, accounting for about half of the total variance of the EASMI. Increased vegetation greenness on the southeastern TP is followed by increased summer rainfall over the southeastern TP, East Asian summer subtropical frontal region and many areas of northern China, and decreased rainfall over western North Pacific summer monsoon region, and vice versa.

[24] We further discuss the possible physical mechanism explaining the close relationship between May vegetation greenness on the southeastern TP and the EASM system. The increased vegetation greenness on the southeastern TP tends to result in higher thermal effects both at the surface and in the troposphere. The thermal effects induced by increased vegetation greenness may subsequently intensify the South Asian high and enhance upper-level anticyclonic circulation, and also increase the southwesterlies over East Asian summer subtropical frontal region. Over the southeastern TP, East Asian summer subtropical frontal region and many areas of northern China, the thermal effects of vegetation greenness on the southeastern TP tends to enhance ascending motion, and strengthen convergence at the lower layers and divergence at the higher layers, resulting in increased summer rainfall. In contrast, opposite changes appear over the western North Pacific, i.e., strengthened descending motion, enhanced divergence at the lower level but enhanced convergence at the upper level, which cause decreased summer rainfall. Previous studies have demonstrated that the heating on the TP has a close linkage with East Asian summer rainfall [e.g., Hsu and Liu, 2003; Zhang et al., 2006; Bao et al., 2008; Wang et al., 2008a]. The pattern of precipitation response to the TP heating largely agrees with our result. The agreement lends support to our finding. Meanwhile, it should be noted that the mechanisms causing the EASM variation and variability can be quite complicated, particularly involving complex ocean-land-atmosphere interactions. Lagged relationships are widely used to infer, but cannot guarantee, the cause and effect of land-atmosphere interaction (and also ocean-atmosphere interaction). The oceanic processes and the snow may influence the relationship between May vegetation greenness on the southeastern TP and the EASM. Therefore, the physical mechanism we propose clearly need to be further tested using more detailed and higher quality data set, and high-resolution model simulations.

[25] This study demonstrates that May NDVI on the southeastern TP is closely associated with the EASMI, suggesting that it can be a useful predictor for the EASM. An empirical model is further established to predict the EASM by the combination of ENSO and May NDVI on the southeastern TP. Hindcast for the period of 1982–2006 shows that ENSO and May NDVI on the southeastern TP together can account for 58% of the observed EASMI variance. However, if May NDVI on the southeastern TP is excluded from the empirical prediction model, the explained variance is reduced to 33%, indicating that May NDVI on the southeastern TP makes an important contribution to the improved prediction skill. Application of May NDVI on the southeastern TP in practical forecast of the EASM

should be recommended, since the NDVI can be easily monitored in advance.

[26] **Acknowledgments.** The source for NDVI data set was the Global Land Cover Facility, University of Maryland. NCEP/DOE reanalysis was produced with the support of the U.S. National Weather Service and of PCMDI (U.S. Department of Energy). This work was supported by the “100-talent program” of the Chinese Academy of Sciences, a special fund for the President’s prize of the Chinese Academy of, and National Basic Research Program of China (2009CB421405).

## References

- Bao, Q., B. Wang, Y. Liu, and G. Wu (2008), The impact of the Tibetan Plateau warming on the East Asian summer monsoon: A study of numerical simulation (in Chinese), *Chin. J. Atmos. Sci.*, *32*(5), 997–1005.
- Betts, R. A. (2001), Biogeophysical impacts of land use on present-day climate: Near-surface temperature change and radiative forcing, *Atmos. Sci. Lett.*, *2*, 39–51, doi:10.1006/asle.2001.0023.
- Blockeel, H., and J. Struyf (2002), Efficient algorithms for decision tree cross-validation, *J. Mach. Learn. Res.*, *3*, 621–650, doi:10.1162/jmlr.2003.3.4-5.621.
- Bonan, G. B. (1997), Effects of land use on the climate of the United States, *Clim. Change*, *37*, 449–486, doi:10.1023/A:1005305708775.
- Bonan, G. B. (2008), *Ecological Climatology*, 2nd ed., 550 pp., Cambridge Univ. Press, Cambridge, U.K.
- Bounoua, L., R. DeFries, G. J. Collatz, P. J. Sellers, and H. Kahn (2002), Effects of land cover conversion on surface climate, *Clim. Change*, *52*, 29–64, doi:10.1023/A:1013051420309.
- Brovkin, V., A. Ganopolski, M. Claussen, C. Kubatzki, and V. Petoukhov (1999), Modelling climate response to historical land cover change, *Global Ecol. Biogeogr.*, *8*, 509–517, doi:10.1046/j.1365-2699.1999.00169.x.
- Brovkin, V., et al. (2006), Biogeophysical effects of historical land cover changes simulated by six Earth system models of intermediate complexity, *Clim. Dyn.*, *26*, 587–600, doi:10.1007/s00382-005-0092-6.
- Cane, M. A., S. E. Zebiak, and S. C. Dolan (1986), Experimental forecasts of El Niño, *Nature*, *321*, 827–832, doi:10.1038/321827a0.
- Castro, C. L., A. B. Beltran-Przekurat, and R. A. Pielke Sr. (2009), Spatio-temporal variability of precipitation, modeled soil moisture, and vegetation greenness in North America within the recent observational record, *J. Hydrometeorol.*, *10*, 1355–1378, doi:10.1175/2009JHM1123.1.
- Chang, C.-P. (2004), Preface, in *East Asian Monsoon*, edited by C.-P. Chang, pp. v–vi, World Sci., Singapore.
- Chase, T. N., J. A. Knaff, R. A. Pielke Sr., and E. Kalnay (2003), Changes in global monsoon circulations since 1950, *Nat. Hazards*, *29*, 229–254, doi:10.1023/A:1023638030885.
- Chen, L., and Z. Yan (1979), *Impact of the snow cover over the Tibetan Plateau in winter and spring on the atmospheric circulation and the precipitation in South China during the rainy season* (in Chinese), *Coll. Pap. Medium-Long-Range Hydrol.-Meteorol. Forecast*, *1*, pp. 185–195, Water Resour. and Elec. Power Press, Beijing.
- Cui, X., H. F. Graf, B. Langmann, W. Chen, and R. Huang (2006), Climate impacts of anthropogenic land use changes on the Tibetan Plateau, *Global Planet. Change*, *54*, 33–56, doi:10.1016/j.gloplacha.2005.07.006.
- Davin, E. L., and N. de Noblet-Ducoudre (2010), Climatic impact of global-scale deforestation: Radiative versus nonradiative processes, *J. Clim.*, *23*, 97–112, doi:10.1175/2009JCLI3102.1.
- Ding, M., Y. Zhang, L. Liu, W. Zhang, Z. Wang, and W. Bai (2007), The relationship between NDVI and precipitation on the Tibetan Plateau, *J. Geogr. Sci.*, *17*, 259–268, doi:10.1007/s11442-007-0259-7.
- Ding, Y. (1992), Summer monsoon rainfalls in China, *J. Meteorol. Soc. Jpn.*, *70*, 373–396.
- Ding, Y., and J. C. L. Chan (2005), The East Asian summer monsoon: An overview, *Meteorol. Atmos. Phys.*, *89*, 117–142, doi:10.1007/s00703-005-0125-z.
- Duan, A., and G. Wu (2005), Role of the Tibetan Plateau thermal forcing in the summer climate patterns over subtropical Asia, *Clim. Dyn.*, *24*, 793–807, doi:10.1007/s00382-004-0488-8.
- Efron, B., and R. Tibshirani (1993), *An Introduction to the Bootstrap*, 436 pp., Chapman and Hall, New York.
- Feddema, J. J., K. W. Oleson, G. B. Bonan, L. Mearns, W. M. Washington, G. Meehl, and D. Nychka (2005), A comparison of a GCM response to historical anthropogenic land cover change and model sensitivity to uncertainty in present-day land cover representations, *Clim. Dyn.*, *25*(6), 581–609, doi:10.1007/s00382-005-0038-z.
- Fu, C. (2003), Potential impacts of human-induced land cover change on East Asia monsoon, *Global Planet. Change*, *37*, 219–229.

- Fu, C., and X. Teng (1988), Relationship between summer climate in China and El Niño/Southern Oscillation phenomenon (in Chinese), *Chin. J. Atmos. Sci.*, *12*, 133–141.
- Gao, X., Y. Luo, W. Lin, Z. Zhao, and F. Giorgi (2003), Simulation of effects of land use change on climate in China by a regional climate model, *Adv. Atmos. Sci.*, *20*, 583–592, doi:10.1007/BF02915501.
- Hahn, D. G., and J. Shukla (1976), An apparent relationship between Eurasian snow cover and Indian monsoon rainfall, *J. Atmos. Sci.*, *33*, 2461–2462, doi:10.1175/1520-0469(1976)033<2461:AARBES>2.0.CO;2.
- Hsu, H. H., and X. Liu (2003), Relationship between the Tibetan Plateau heating and East Asian summer monsoon rainfall, *Geophys. Res. Lett.*, *30*(20), 2066, doi:10.1029/2003GL017909.
- Hua, W., G. Fan, D. Zhou, C. Ni, X. Li, Y. Wang, Y. Liu, and X. Huang (2008), Preliminary analysis on the relationships between Tibetan Plateau NDVI change and its surface heat source and precipitation of China, *Sci. China Ser. D*, *51*, 677–685, doi:10.1007/s11430-008-0063-y.
- Huang, R., and Y. Wu (1989), The influence of ENSO on the summer climate change in China and its mechanism, *Adv. Atmos. Sci.*, *6*, 21–32, doi:10.1007/BF02656915.
- Huang, R., L. Zhou, and W. Chen (2003), The progresses of recent studies on the variabilities of the East Asian monsoon and their causes, *Adv. Atmos. Sci.*, *20*, 55–69.
- Kanamitsu, M., W. Ebisuzaki, J. Woollen, S.-K. Yang, J. J. Hnilo, M. Fiorino, and G. L. Potter (2002), NCEP–DEO AMIP–II Reanalysis (R-2), *Bull. Am. Meteorol. Soc.*, *83*, 1631–1643, doi:10.1175/BAMS-83-11-1631(2002)083<1631:NAR>2.3.CO;2.
- Kang, I.-S., et al. (2002), Intercomparison of the climatological variations of Asian summer monsoon precipitation simulated by 10 GCMs, *Clim. Dyn.*, *19*, 383–395, doi:10.1007/s00382-002-0245-9.
- Kaufmann, R. K., L. Zhou, R. B. Myneni, C. J. Tucker, D. Slayback, N. V. Shabanov, and J. Pinzon (2003), The effect of vegetation on surface temperature: A statistical analysis of NDVI and climate data, *Geophys. Res. Lett.*, *30*(22), 2147, doi:10.1029/2003GL018251.
- Koster, R. D., and M. J. Suarez (1995), Relative contributions of land and ocean processes to precipitation variability, *J. Geophys. Res.*, *100*, 13,775–13,790, doi:10.1029/95JD00176.
- Kutzbach, J., G. Bonan, J. Foley, and S. P. Harrison (1996), Vegetation and soil feedbacks on the response of the African monsoon to orbital forcing in the early to middle Holocene, *Nature*, *384*, 623–626, doi:10.1038/384623a0.
- Lau, K.-M., and H. Weng (2001), Coherent modes of global SST and summer rainfall over China: An assessment of the regional impacts of the 1997–98 El Niño, *J. Clim.*, *14*, 1294–1308, doi:10.1175/1520-0442(2001)014<1294:CMOGSA>2.0.CO;2.
- Lee, E.-J., J.-G. Jhun, and C.-K. Park (2005), Remote connection of the northeast Asian summer rainfall variation revealed by a newly defined monsoon index, *J. Clim.*, *18*, 4381–4393, doi:10.1175/JCLI3545.1.
- Lee, E., T. N. Chase, and B. Rajagopalan (2008), Highly improved predictive skill in the forecasting of the East Asian summer monsoon, *Water Resour. Res.*, *44*, W10422, doi:10.1029/2007WR006514.
- Liu, Z. Y., M. Notaro, J. Kutzbach, and N. Liu (2006), Assessing global vegetation–climate feedbacks from observations, *J. Clim.*, *19*, 787–814, doi:10.1175/JCLI3658.1.
- Liu, Y. M., Q. Bao, A. M. Duan, Z. A. Qian, and G. X. Wu (2007), Recent progress in the impact of the Tibetan Plateau on climate in China, *Adv. Atmos. Sci.*, *24*, 1060–1076, doi:10.1007/s00376-007-1060-3.
- Los, S. O., G. P. Weedon, P. R. J. North, J. D. Kaduk, C. M. Taylor, and P. M. Cox (2006), An observation-based estimate of the strength of rainfall–vegetation interactions in the Sahel, *Geophys. Res. Lett.*, *33*, L16402, doi:10.1029/2006GL027065.
- Ma, Y., et al. (2009), Recent advances on the study of atmosphere–land interaction observations on the Tibetan Plateau, *Hydrol. Earth Syst. Sci.*, *13*, 1103–1111, doi:10.5194/hess-13-1103-2009.
- Nemani, R. R., C. D. Keeling, H. Hashimoto, W. M. Jolly, S. C. Piper, C. J. Tucker, R. B. Myneni, and S. W. Running (2003), Climate-driven increases in global terrestrial net primary production from 1982 to 1999, *Science*, *300*, 1560–1563, doi:10.1126/science.1082750.
- Notaro, M., Z. Liu, and J. W. Williams (2006), Observed vegetation–climate feedbacks in the United States, *J. Clim.*, *19*, 763–786, doi:10.1175/JCLI3657.1.
- Peng, S., S. Piao, P. Ciais, J. Fang, and X. Wang (2010), Change in winter snow depth and its impacts on vegetation in China, *Global Change Biol.*, doi:10.1111/j.1365-2486.2010.02210.x.
- Pielke, R. A., Sr. (2001), Influence of the spatial distribution of vegetation and soils on the prediction of cumulus convective rainfall, *Rev. Geophys.*, *39*, 151–177, doi:10.1029/1999RG000072.
- Pielke, R. A., Sr., R. Avissar, M. Raupach, A. J. Dolman, X. Zeng, and A. S. Denning (1998), Interactions between the atmosphere and terrestrial ecosystems: Influence on weather and climate, *Global Change Biol.*, *4*, 461–475, doi:10.1046/j.1365-2486.1998.t01-1-00176.x.
- Pinzon, J., M. E. Brown, and C. J. Tucker (2004), Satellite time series correction of orbital drift artifacts using empirical mode decomposition, in *Hilbert–Huang Transform: Introduction and Applications*, edited by N. E. Huang, pp. 173–176, NASA Goddard Space Flight Cent., Greenbelt, Md.
- Qian, Y., Y. Zheng, Y. Zhang, and M. Miao (2003), Responses of China’s summer monsoon climate to snow anomaly over the Tibetan Plateau, *Int. J. Climatol.*, *23*, 593–613, doi:10.1002/joc.901.
- Shukla, J. (1998), Predictability in the midst of chaos: A scientific basis for climate forecasting, *Science*, *282*, 728–731, doi:10.1126/science.282.5389.728.
- Shukla, J., and Y. Mintz (1982), Influence of land-surface evapotranspiration on the Earth’s climate, *Science*, *215*, 1498–1501, doi:10.1126/science.215.4539.1498.
- Stone, M. (1974), Cross-validation choice and the assessment of statistical predictions, *J. R. Stat. Soc. B*, *36*(1), 111–147.
- Takata, K., K. Saito, and T. Yasunari (2009), Changes in the Asian monsoon climate during 1700–1850 induced by preindustrial cultivation, *Proc. Natl. Acad. Sci. U. S. A.*, *106*, 9586–9589, doi:10.1073/pnas.0807346106.
- Tao, S., and L. Chen (1987), A review of recent research of the East Asian summer monsoon in China, in *Monsoon Meteorology*, edited by C. Chang and T. N. Krishnamurti, pp. 60–92, Oxford Univ. Press, New York.
- Tucker, C. J., I. Fung, C. Keeling, and R. Gammon (1986), Relationship between atmospheric CO<sub>2</sub> variations and satellite-derived vegetation index, *Nature*, *319*, 195–199, doi:10.1038/319195a0.
- Tucker, C. J., J. E. Pinzon, M. E. Brown, D. Slayback, E. W. Pak, and R. Mahoney (2005), An extended AVHRR 8-km NDVI data set compatible with MODIS and spot vegetation NDVI data, *Int. J. Remote Sens.*, *26*, 4485–4498, doi:10.1080/01431160500168686.
- Ueda, H., M. Shinoda, and H. Kamahori (2003), Spring northward retreat of Eurasian snow cover relevant to seasonal and interannual variations of atmospheric circulation, *Int. J. Climatol.*, *23*, 615–629, doi:10.1002/joc.903.
- von Storch, H., and F. W. Zwiers (1999), *Statistical Analysis in Climate Research*, 499 pp., Cambridge Univ. Press, New York, doi:10.1017/CBO9780511612336.
- Wang, B., and Z. Fan (1999), Choice of South Asian summer monsoon indices, *Bull. Am. Meteorol. Soc.*, *80*, 629–638, doi:10.1175/1520-0477(1999)080<0629:COSASM>2.0.CO;2.
- Wang, B., and T. Li (2004), East Asian monsoon and ENSO interaction, in *East Asian Monsoon*, edited by C.-P. Chang, pp. 172–212, World Sci., Singapore.
- Wang, B., R. Wu, and X. Fu (2000), Pacific–East Asian teleconnection: How does ENSO affect East Asian climate?, *J. Clim.*, *13*, 1517–1536, doi:10.1175/1520-0442(2000)013<1517:PEATHD>2.0.CO;2.
- Wang, B., Q. Ding, X. Fu, I.-S. Kang, K. Jin, J. Shukla, and F. Doblas-Reyes (2005), Fundamental challenge in simulation and prediction of summer monsoon rainfall, *Geophys. Res. Lett.*, *32*, L15711, doi:10.1029/2005GL022734.
- Wang, B., Q. Bao, B. Hoskins, G. Wu, and Y. Liu (2008a), Tibetan Plateau warming and precipitation changes in East Asia, *Geophys. Res. Lett.*, *35*, L14702, doi:10.1029/2008GL034330.
- Wang, B., Z. Wu, J. Li, J. Liu, C.-P. Chang, Y. Ding, and G. Wu (2008b), How to measure the strength of the East Asian summer monsoon?, *J. Clim.*, *21*, 4449–4463, doi:10.1175/2008JCLI2183.1.
- Wang, B., et al. (2009a), Advance and prospectus of seasonal prediction: Assessment of the APCC/CLIPAS 14-model ensemble retrospective seasonal prediction (1980–2004), *Clim. Dyn.*, *33*, 93–117, doi:10.1007/s00382-008-0460-0.
- Wang, B., J. Liu, J. Yang, T. Zhou, and Z. Wu (2009b), Distinct principal modes of early and late summer rainfall anomalies in East Asia, *J. Clim.*, *22*, 3864–3875, doi:10.1175/2009JCLI2850.1.
- Wang, W., T. B. Anderson, N. Phillips, K. R. Kaufman, C. Potter, and R. B. Myneni (2006), Feedbacks of vegetation on summertime climate variability over the North American grasslands. Part I: Statistical analysis, *Earth Interact.*, *10*(17), 1–27, doi:10.1175/EI196.1.
- Wang, Y., P. Zhao, R. Yu, and G. Rasul (2010), Inter-decadal variability of Tibetan spring vegetation and its associations with eastern China spring rainfall, *Int. J. Climatol.*, *30*, 856–865.
- Webster, P. J. (1987), The elementary monsoons, in *Monsoons*, edited by J. F. Fein and P. L. Stephens, pp. 3–32, John Wiley, New York.
- Wei, L., and D. Li (2003), Evaluation of NCEP/DOE surface flux data over Qinghai–Xizang Plateau (in Chinese), *Plateau Meteorol.*, *22*, 478–487.
- Weng, H.-Y., K.-M. Lau, and Y. Xue (1999), Multi-scale summer rainfall variability over China and its long-term link to global sea surface temperature variability, *J. Meteorol. Soc. Jpn.*, *77*, 845–857.
- Wu, G., W. Li, H. Guo, H. Liu, J. Xue, and Z. Wang (1997), Sensible heat-driven air-pump over the Tibetan Plateau and its impact on the Asian summer monsoon (in Chinese), in *Collections on the Memory of Zhao Juzhang*, edited by T. C. Ye, pp. 116–126, Chin Sci. Press, Beijing.

- Wu, G. X., Y. M. Liu, X. Liu, A. M. Duan, and X. Y. Liang (2005), How the heating over the Tibetan Plateau affects the Asian climate in summer (in Chinese), *Chin. J. Atmos. Sci.*, *29*, 47–56.
- Wu, R., and B. P. Kirtman (2007), Observed relationship of spring and summer East Asian rainfall with winter and spring Eurasian snow, *J. Clim.*, *20*, 1285–1304, doi:10.1175/JCLI4068.1.
- Wu, T., and Z. Qian (2003), The relation between the Tibetan winter snow and the Asian summer monsoon and rainfall: An observational investigation, *J. Clim.*, *16*, 2038–2051, doi:10.1175/1520-0442(2003)016<2038:TRBTTW>2.0.CO;2.
- Wu, W., and R. E. Dickinson (2004), Time scales of layered soil moisture memory in the context of land-atmosphere interaction, *J. Clim.*, *17*, 2752–2764, doi:10.1175/1520-0442(2004)017<2752:TSOLSM>2.0.CO;2.
- Wu, Z., B. Wang, J. Li, and F.-F. Jin (2009), An empirical seasonal prediction model of the East Asian summer monsoon using ENSO and NAO, *J. Geophys. Res.*, *114*, D18120, doi:10.1029/2009JD011733.
- Xie, P., and P. A. Arkin (1997), Global precipitation: A 17-year monthly analysis based on gauge observations, satellite estimates, and numerical model outputs, *Bull. Am. Meteorol. Soc.*, *78*, 2539–2558, doi:10.1175/1520-0477(1997)078<2539:GPAYMA>2.0.CO;2.
- Xie, S.-P., K. Hu, J. Hafner, H. Tokinaga, Y. Du, G. Huang, and T. Sampe (2009), Indian Ocean capacitor effect on Indo-western Pacific climate during the summer following El Niño, *J. Clim.*, *22*, 730–747, doi:10.1175/2008JCLI2544.1.
- Xu, L., and Y. Li (2010), Reexamining the impact of Tibetan snow anomalies to the East Asian summer monsoon using MODIS snow retrieval, *Clim. Dyn.*, *35*, 1039–1053.
- Xu, M., C.-P. Chang, C. Fu, Y. Qi, A. Robock, D. Robinson, and H. Zhang (2006), Steady decline of East Asian monsoon winds, 1969–2000: Evidence from direct ground measurements of wind speed, *J. Geophys. Res.*, *111*, D24111, doi:10.1029/2006JD007337.
- Xu, X., and Z. Lin (2002), Remote sensing retrieval of surface monthly mean albedo in Qinghai-Xizang Plateau (in Chinese), *Plateau Meteorol.*, *21*, 233–237.
- Xue, Y. (1996), The impact of desertification in the Mongolian and the inner Mongolian grassland on the regional climate, *J. Clim.*, *9*, 2173–2189, doi:10.1175/1520-0442(1996)009<2173:TIODIT>2.0.CO;2.
- Xue, Y., H.-M. H. Juang, W.-P. Li, S. Prince, R. DeFries, Y. Jiao, and R. Vasic (2004), Role of land surface processes in monsoon development: East Asia and West Africa, *J. Geophys. Res.*, *109*, D03105, doi:10.1029/2003JD003556.
- Xue, Y., F. De Sales, R. Vasic, C. R. Mechoso, A. Arakawa, and S. Prince (2010), Global and seasonal assessment of interactions between climate and vegetation biophysical processes: A GCM study with different land-vegetation representations, *J. Clim.*, *23*, 1411–1433, doi:10.1175/2009JCLI3054.1.
- Yanai, M., and G. Wu (2006), Effects of the Tibetan Plateau, in *The Asian Monsoon*, edited by B. Wang, pp. 513–549, Springer, New York, doi:10.1007/3-540-37722-0\_13.
- Yang, J., Q. Liu, S.-P. Xie, Z. Liu, and L. Wu (2007), Impact of the Indian Ocean SST basin mode on the Asian summer monsoon, *Geophys. Res. Lett.*, *34*, L02708, doi:10.1029/2006GL028571.
- Ye, D., and Y. Gao (1979), *The Meteorology of the Qinghai-Xizang (Tibet) Plateau* (in Chinese), Sci. Press, Beijing.
- Yeh, T., T. Wetherald, and S. Manabe (1984), The effect of soil moisture on the short-term climate and hydrology change: A numerical experiment, *Mon. Weather Rev.*, *112*, 474–490, doi:10.1175/1520-0493(1984)112<0474:TEOSMO>2.0.CO;2.
- Zhang, J., W. Dong, C. Fu, and L. Wu (2003a), The influence of vegetation cover on summer precipitation in China: A statistical analysis of NDVI and climate data, *Adv. Atmos. Sci.*, *20*, 1002–1006, doi:10.1007/BF02915523.
- Zhang, J., W. Dong, D. Ye, and C. Fu (2003b), New evidence for effects of land cover in China on summer climate, *Chin. Sci. Bull.*, *48*, 401–405, doi:10.1360/03tb9084.
- Zhang, J., W.-C. Wang, and J. Wei (2008), Assessing land-atmosphere coupling using soil moisture from the Global Land Data Assimilation System and observational precipitation, *J. Geophys. Res.*, *113*, D17119, doi:10.1029/2008JD009807.
- Zhang, Q. Y., Z. H. Jin, and J. B. Peng (2006), The relationship between convection over the Tibetan Plateau and circulation over East Asia (in Chinese), *Chin. J. Atmos. Sci.*, *30*, 802–812.
- Zhang, Y., T. Li, and B. Wang (2004), Decadal change of the spring snow depth over the Tibetan Plateau: The associated circulation and influence on the East Asian summer monsoon, *J. Clim.*, *17*, 2780–2793, doi:10.1175/1520-0442(2004)017<2780:DCOTSS>2.0.CO;2.
- Zhao, P., and L. Chen (2001), Climate features of atmospheric heat source/sink over the Qinghai-Xizang Plateau in 35 years and its relation to rainfall in China, *Sci. China Ser. D*, *44*(9), 858–864.
- Zheng, D. (1996), The system of physico-geographical regions of the Qinghai-Xizang (Tibet) Plateau, *Sci. China Ser. D*, *39*, 410–417.
- Zhou, L., C. J. Tucker, R. K. Kaufmann, D. Slayback, N. V. Shabanov, and R. B. Myneni (2001), Variations in northern vegetation activity inferred from satellite data of vegetation index during 1981 to 1999, *J. Geophys. Res.*, *106*, 20,069–20,083, doi:10.1029/2000JD000115.
- Zuo, Z., R. Zhang, and P. Zhao (2010), The relation of vegetation over the Tibetan Plateau to rainfall in China during the boreal summer, *Clim. Dyn.*, *35*, doi:10.1007/s00382-010-0863-6.

G. Huang, LASG and RCE-TEA, Institute of Atmospheric Physics, Chinese Academy of Sciences, Beijing 100029, China.

L. Wu and J. Zhang, Center for Monsoon System Research, Institute of Atmospheric Physics, Chinese Academy of Sciences, Beijing 100029, China. (zjy@mail.iap.ac.cn)

Y. Zhang, GEST, University of Maryland Baltimore County, 5523 Research Park Dr., Ste. 320, Baltimore, MD 21228, USA.

W. Zhu, State Key Laboratory of Earth Surface Processes and Resource Ecology, Beijing Normal University, Beijing 100875, China.